Langmuir

Research Article

Nanostructured Ultrathin Films of Alternating Sexithiophenes and Electropolymerizable Polycarbazole Precursor Layers Investigated by Electrochemical Surface Plasmon Resonance (EC-SPR) Spectroscopy

Saengrawee Sriwichai, Akira Baba, Suxiang Deng, Chengyu Huang, Sukon Phanichphant, and Rigoberto C. Advincula

Langmuir, **2008**, 24 (16), 9017-9023 • DOI: 10.1021/la800307u • Publication Date (Web): 11 July 2008

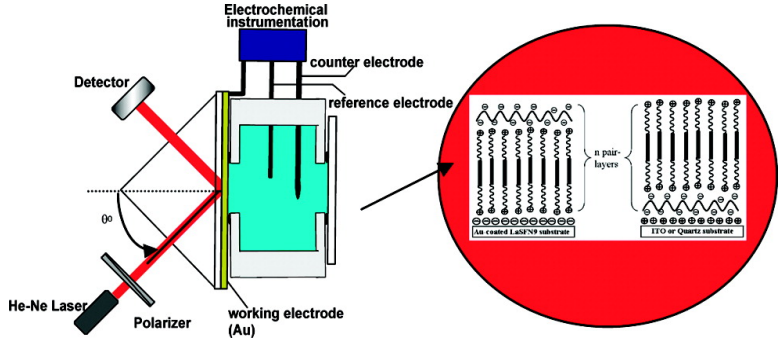

More About This Article

Additional resources and features associated with this article are available within the HTML version:

- Supporting Information
- Access to high resolution figures
- Links to articles and content related to this article
- Copyright permission to reproduce figures and/or text from this article

View the Full Text HTML

Nanostructured Ultrathin Films of Alternating Sexithiophenes and Electropolymerizable Polycarbazole Precursor Layers Investigated by Electrochemical Surface Plasmon Resonance (EC-SPR) Spectroscopy

Saengrawee Sriwichai,[†,‡] Akira Baba,[†] Suxiang Deng,[†] Chengyu Huang,[†] Sukon Phanichphant,*[,‡] and Rigoberto C. Advincula*[,†]

Departments of Chemistry and Chemical Engineering, University of Houston, Houston, Texas 77204-5003, and Department of Chemistry, Faculty of Science, Chiang Mai University, Chiang Mai, 50200 Thailand

Received January 29, 2008. Revised Manuscript Received May 11, 2008

Nanostructured ultrathin films of linear and dendrimeric cationic sexithiophenes, 6TNL and 6TND, respectively, alternated with anionic polycarbazole precursor, poly(2-(*N*-carbazolyl) ethyl methacrylate-*co*-methacrylic acid) or PCEMMA32, were successfully fabricated using the layer-by-layer self-assembly deposition technique. The two electro-optically active oligomers exhibited distinct optical properties and aggregation behavior in solution and films as studied by UV−vis and fluorescence spectroscopy. The stepwise increase of the 6TNL/PCEMMA32 and 6TND/PCEMMA32 layers was confirmed by UV−vis spectroscopy and in situ surface plasmon resonance (SPR) spectroscopy. The intralayer electrochemical polymerization and cross-linking behavior of the carbazole functionalized PCEMMA32 layers were then investigated using cyclic voltammetry (CV) and electrochemical surface plasmon resonance (EC-SPR) spectroscopy. The increase in current with each cycle confirmed intralayer cross-linking followed by the doping−dedoping process within these films. The two types of films differed with respect to dielectric constant and thickness changes before and after electropolymerization, indicating the influence of the oligothiophene layers. This demonstrated for the first time the preparation of highly ordered organic semiconductors alternated with in situ electropolymerizable layers in ultrathin films.

Introduction

Oligothiophenes and polythiophenes have been extensively and intensively studied as materials for electro-optical and electronic devices, for example, light-emitting diodes (LEDs) and field effect transistors (FETs).[1] Among the oligothiophenes, the linear quinquethiophenes (5T) and sexithiophenes (6T) are of interest due to their high charge mobilities and ability to form ordered structures for high-performance organic thin film devices.[2] Garnier et al.[3] first demonstrated sexithiophene films with very high hole mobility due to the high $\pi-\pi$ stacking order and domain formation. The main problem for the 6T molecule is its poor solubility in most organic solvents. Therefore, they have been modified with alkyl chain substituents in the α,ω position to increase their solubility in organic solvents.[4] The introduction of quaternary amine end-groups on the alkyl substituted 6T enabled solubility to water and a variety of polar solvents.[5] This in turn allowed the preparation of various alternating layer-by-layer nanostructured ultrathin films incorporating the high mobility oligomers with various polyelectrolytes and even clay.[5] The solution aggregation behavior of this linear 6T bolaform amphiphile has also been studied.[5a] In addition to linear oligomers, electro-optically active dendrimers are also of great interest because of their different topological and packing behavior in thin films.[6] For example, the Advincula group has reported the synthesis and characterization of thiophene dendrimers and their ability to form nanostructures on surfaces.[7] However, up to now, no nanostructured layered ultrathin films incorporating dendrimeric oligothiophenes have been reported.

Poly(*N*-vinylcarbazole) (PVK) is a well-known material for use as a hole transport layer in organic devices and as a precursor polymer.[8] This material exhibits interesting electrical and optical properties which have important applications for the fabrication of organic-semiconductor devices such as solar cells and light-emitting diodes.[9] Furthermore, the electrochemically polymerized PVK can exhibit interesting electrochromic properties in the presence of π-conjugated 3,6-linkages (formation of polycarbazole).[10] Polycarbazole itself has been extensively studied for use in electrically conducting and electrochromic devices.[11] Recently, our group has demonstrated a novel method for conversion of "precursor polymers" to form conjugated polymer networks (CPNs) or cross-linked films

* To whom correspondence should be addressed. E-mail: radvincula@uh.edu (R.C.A.) or sukon@science.cmu.ac.th (S.P.).

† University of Houston.

‡ Chiang Mai University.

(1) (a) Meller, L. L.; Yu, Y. *J. Org. Chem.* **1995**, *60*, 6813. (b) Ong, B. S.; Wu, Y.; Liu, P.; Gardner, S. *J. Am. Chem. Soc.* **2004**, *126*, 3378. (c) Kline, R. J.; McGehee, M. D.; Kadnikova, E. N.; Liu, J.; Frechet, J. M. J. *Adv. Mater.* **2003**, *15*, 1519.

(2) (a) Melucci, M.; Barbarella, G.; Zambianchi, M.; Di Pietrio, P.; Bongini, A. *J. Org. Chem.* **2004**, *69*, 4821. (b) Murphy, A. R.; Frechet, J. M. J.; Chang, P.; Lee, J.; Subramanian, V. *J. Am. Chem. Soc.* **2004**, *126*, 1596.

(3) Garnier, F.; Horowitz, G.; Peng, X. Z.; Fichou, D. *Synth. Met.* **1991**, *45*, 163.

(4) Delabouglise, D.; Hmyene, M.; Horowitz, G.; Yassar, A.; Garnier, F. *Adv. Mater.* **1992**, *4*, 107.

(5) (a) Xia, C.; Locklin, J.; Youk, J. H.; Fulghum, T.; Advincula, R. C. *Langmuir* **2002**, *18*, 955. (b) Locklin, J.; Youk, J. H.; Xia, C.; Park, M.-K.; Fan, X.; Advincula, R. C. *Langmuir* **2002**, *18*, 877. (c) Fan, X.; Locklin, J.; Youk, J. H.; Blanton, W.; Xia, C.; Advincula, R. *Chem. Mater.* **2002**, *14*, 2184. (d) Baba, A.; Locklin, J.; Xu, R.; Advincula, R. *J. Phys. Chem. B* **2006**, *110*, 42–45. (e) Xia, C.; Locklin, J.; Youk, J.; Fulghum, T.; Advincula, R. *Langmuir* **2002**, *18*(3), 955–957.

(6) (a) Wang, S.; Hong, J. W.; Bazan, G. C. *Org. Lett.* **2005**, *7*, 1907. (b) Schenning, A. P. H. J.; Peeters, E.; Meijer, E. W. *J. Am. Chem. Soc.* **2000**, *122*, 4489.

(7) (a) Xia, C.; Fan, X.; Locklin, J.; Advincula, R. C.; Gies, A.; Nonidez, W. *J. Am. Chem. Soc.* **2004**, *126*, 8735. (b) Xia, C.; Fan, X.; Locklin, J.; Advincula, R. C. *Org. Lett.* **2002**, *4*, 2067.

(8) Mort, J., Pfister, G., Eds.; *Electronic Properties of Polymers*; Wiley-Interscience: New York, 1982; pp 215−265.

(9) (a) Mori, T.; Obata, K.; Imaizumi, K.; Mizutani, T. *Appl. Phys. Lett.* **1996**, *69*, 3309. (b) Michelotti, F.; Borghese, F.; Bertolotti, M.; Cianci, E.; Foglietti, V. *Synth. Met.* **2000**, *111*, 105.

(10) Romero, D.; Nuesch, F.; Benazzi, T.; Ades, D.; Stove, A.; Zuppiroli, L. *Adv. Mater.* **1997**, *9*, 1158.

(11) Desbene-Monvernay, A.; Dubois, J. E.; Lacaze, P. C. *J. Electroanal. Chem.* **1985**, *189*, 51.

10.1021/la800307u CCC: $40.75
Published on Web 07/11/2008

on flat electrode substrates.[12] In this approach, a precursor polymer is first synthesized chemically and by design contains pendant electroactive monomer units. Electropolymerization or chemical oxidation results in a conjugated polymer network having both inter- and intramolecular cross-linking possibilities between the pendant electroactive units. This process is of high interest for depositing insoluble ultrathin films of conjugated polymer (or oligomer) species for practical electro-optical applications in devices. A number of combinations are possible for the design of these precursor polymer backbones and electroactive monomer units. Extensive studies have been reported by the Advincula group for carbazole containing precursor polymers.[12]

The layer-by-layer (LbL) self-assembly technique has become a powerful and versatile method for fabrication of nanostructured ultrathin films with uniform and controlled thickness.[13] The process involves alternate and sequential adsorption of polycationic and polyanionic molecules from solution to charged surfaces as driven by electrostatic interaction. This method has been widely used for layered assembly of conjugated polymers and nanoparticles in applications such as semiconductor devices,[14] sensors,[15] and DNA delivery.[16] Furthermore, the evaluation of film formation and electrochemical properties of LbL conjugated molecule films is also important.[17] Surface plasmon resonance (SPR) and Electrochemical surface plasmon resonance (EC-SPR) spectroscopy are highly sensitive techniques for characterization and study of interfaces and ultrathin films prepared by the LbL method.[18,19] The combination of SPR and electrochemical methods has become a powerful technique for simultaneous observation of optical and electrochemical properties at substrate/electrolyte interfaces.[19] Information about film formation and optical property changes can be obtained by simultaneously monitoring angular-reflectivity changes with current or potential.[20] The characterization of conducting polymer thin films using EC-SPR spectroscopy has been previously demonstrated.[21] The EC-SPR spectroscopy technique has also been used for many applications including biosensor development[22] and new in situ imaging instruments.[23] Moreover, the electropolymerization of PVK to form conjugated polycarbazole networks have also been investigated using in situ EC-SPR spectroscopy.[24]

In this study, two types of cationic water-soluble sexithiophene (linear and dendrimeric, 6TNL and 6TND, respectively) oligomers were studied for their ability to form nanostructured LbL ultrathin films with a polycarbazole precursor, poly(2-(*N*-carbazolyl) ethyl methacrylate-*co*-methacrylic acid) or PCEMMA32. The two oligomers 6TNL and 6TND were observed to have distinct aggregation behavior in solution and films. The film growth was monitored by UV−vis spectroscopy and in situ SPR spectroscopy. The differences in film forming properties of the two oligomeric topologies were investigated. The sandwiched PCEMMA32 were then electrochemically polymerized and cross-linked by cyclic voltammetry. Their polymerizability and doping-dedoping properties were investigated by in situ EC-SPR spectroscopy.[25]

Experimental Section

Materials. All the chemicals were purchased from Aldrich and used without further purification. Tetrahydrofuran (THF) and toluene were freshly distilled from sodium benzophenone ketyl. Tetrabutylammonium hexafluorophosphate ($TBAPF_6$; Aldrich) was freshly dried under vacuum at about 40 °C. Anhydrous acetonitrile was used as received. The structures of the oligomers and polyelectrolyte used in this experiment are shown in Figure 1.

Synthesis of Cationic Water-Soluble Sexithiophenes. The details for the synthesis of linear cationic water-soluble sexithiophene [5,5′′′′-di((6-(trimethylamino)hexyl)-2,2′:5′,2′′-terthiophene) 2,2′:5′,2′′:5′′,2′′′:5′′′,2′′′′:5′′′′,2′′′′′-sexithiophene, 6TNL] had been reported previously by our group.[5] The synthesis of dendrimeric cationic water-soluble sexithiophenes [6TND] was carried out as shown in Figure 2. More details of the synthesis can be found in the Supporting Information. All of the reactions were carried out under nitrogen atmosphere. The 6TNL and 6TND were obtained by treatment of bromide terminated groups with trimethylamine in ethanol for 1 week.[5]

Synthesis of Polycarbazole Precursor. The details for the synthesis of poly(2-(*N*-carbazolyl) ethyl methacrylate-*co*-methacrylic acid), PCEMMA32, have been described elsewhere.[26]

Layer-by-Layer Adsorption. Quartz, indium tin oxide (ITO), and high refractive index LaSFN9 glass substrates were cleaned by consecutive sonication at 15 min each in the following order: sonicating solution (2% glass cleaning solution), deionized water (resistivity 18.2 MΩ·cm), isopropanol, and acetone. They were then cleaned by argon ion plasma treatment for 5 min. The gold films were vacuum evaporated onto high reflective index LaSFN9 glass substrates (with an adhesion layer of 2 nm Cr, previously evaporated on glass). The thickness of the gold film was ∼45 nm. The substrates were then treated with 1 mM 3-mercapto-1-propanesulfonic acid sodium salt in ethanol for 90 min and finally rinsed with ethanol. The ITO substrate was pretreated with the RCA recipe[27] (H_2O/H_2O_2/NH_3, 5/1/0.3) at 50−60 °C for 75 min and then rinsed with Millipore water. After complete drying, the ITO substrate was treated with 0.5% 3-aminopropyltriethoxysilane (APS) in freshly distilled toluene at 95 °C for 2 h. The substrates were then rinsed with toluene and methanol. The quartz substrate was pretreated with piranha solution (H_2O_2/H_2SO_4, 30/70 v/v) for 30 min and subsequently rinsed with Millipore water. After complete drying, the substrates were functionalized by immersion in 0.5% APS in freshly distilled toluene for 30 min and rinsed with toluene and acetone. The slides were then stored overnight in 0.1 M HCl. The LbL deposition process was performed mainly using the following steps: (1) The functionalized substrates were immersed into a solution of PCEMMA32 (1 mg/mL in dimethyl sulfoxide (DMSO)/water, 2/3 at pH 10) for 10 min and

(12) (a) Xia, C.; Advincula, R. *Chem. Mater.* **2001**, *13*, 1682. (b) Xia, C.; Fan, X.; Park, M.-K.; Advincula, R. C. *Langmuir* **2001**, *17*, 7893. (c) Inaoka, S.; Advincula, R. *Macromolecules* **2002**, *35*, 2426. (d) Taranekar, P.; Fan, X.; Advincula, R. *Langmuir* **2002**, *18*, 7943. (e) Deng, S.; Advincula, R. C. *Chem. Mater.* **2002**, *14*, 4073. (f) Taranekar, P.; Baba, A.; Fulghum, T. M.; Advincula, R. *Macromolecules* **2005**, *38*, 3679.

(13) Decher, G. *Science* **1997**, *277*, 1232.

(14) (a) Ho, P. K. H.; Kim, J.-S.; Burroughes, J. H.; Becker, H.; Li, S. F. Y.; Brown, T. M.; Cacialli, F.; Friend, R. H. *Nature* **2000**, *404*, 481. (b) Advincula, R. C.; Knoll, W.; Frank, C. W.; Roitman, D.; Moon, R.; Sheats, J. *Mater. Res. Soc. Symp. Proc.* **1998**, 115. (c) Patton, D.; Locklin, J.; Meredith, M.; Xin, Y.; Advincula, R. *Chem. Mater.* **2004**, *16*, 5063–5070. (d) Jiang, G.; Baba, A.; Advincula, R. *Langmuir* **2007**, *23*, 817–825.

(15) (a) Rubinstein, I.; Steinberg, S.; Tor, Y.; Shanzer, A.; Sagiv, J. *Nature* **1988**, *332*, 426. (b) Park, M.-K.; Deng, S.; Advincula, R. *J. Am. Chem. Soc.* **2004**, *126*, 13723–13731. (c) Park, M.-K.; Advincula, R. *Langmuir* **2002**, *18*, 4532–4535.

(16) Lvov, Y.; Decher, G.; Sukhorukov, G. *Macromolecules* **1993**, *26*, 5396.

(17) Knoll, W. *Curr. Opin. Colloid Interface Sci.* **1996**, *1*, 137.

(18) (a) Knoll, W. *Annu. Rev. Phys. Chem.* **1998**, *49*, 569. (b) Advincula, R.; Aust, E.; Meyer, W.; Knoll, W. *Langmuir* **1996**, *12*, 3536.

(19) (a) Badia, A.; Arnold, S.; Scheumann, V.; Zizlsperger, M.; Mack, J.; Jung, G.; Knoll, W. *Sens. Actuators, B* **1999**, *54*, 145. (b) Baba, A.; Tian, S.; Stefani, F.; Xia, C.; Wang, Z.; Advincula, R. C.; Johannsmann, D.; Knoll, W. *J. Electroanal. Chem.* **2004**, *562*, 95.

(20) Xia, C.; Advincula, R. C.; Baba, A.; Knoll, W. *Langmuir* **2002**, *18*, 3555.

(21) (a) Raitman, O.; Katz, E.; Willner, I.; Chegel, V.; Popova, G. *Angew. Chem., Int. Ed.* **2001**, *40*, 3649. (b) Kang, X.; Jin, Y.; Chen, G.; Dong, S. *Langmuir* **2002**, *18*, 1713. (c) Baba, A.; Advincula, R. C.; Knoll, W. In *Novel Methods to Study Interfacial Layers*; Möbius, D., Miller, R., Eds.; Studies in Interface Science; Elsevier Science: New York, 2001; Vol. *11*, p 55.

(22) (a) Raitman, O. A.; Katz, E.; Buckmann, A. F.; Willner, I. *J. Am. Chem. Soc.* **2002**, *124*, 6487. (b) Tian, S.; Baba, A.; Liu, J.; Wang, Z.; Knoll, W.; Park, M.-K.; Advincula, R. *Adv. Funct. Mater.* **2003**, *13*, 473.

(23) Baba, A.; Knoll, W.; Advincula, R. *Rev. Sci. Instrum.* **2006**, *77*, 064101.

(24) Baba, A.; Onishi, K.; Knoll, W.; Advincula, R. C. *J. Phys. Chem. B* **2004**, *108*, 18949.

(25) Taranekar, P.; Fulghum, T.; Baba, A.; Patton, D.; Advincula, R. C. *Langmuir* **2007**, *23*, 908.

(26) Waenkaew, P.; Taranekar, P.; Phanichphant, P.; Advincula, R. *Macromol. Rapid Commun.* **2007**, *28*, 1522–1527.

(27) Magnus, P.; Friend, R.; Greenham, N. *Adv. Mater.* **1998**, *10*, 769.

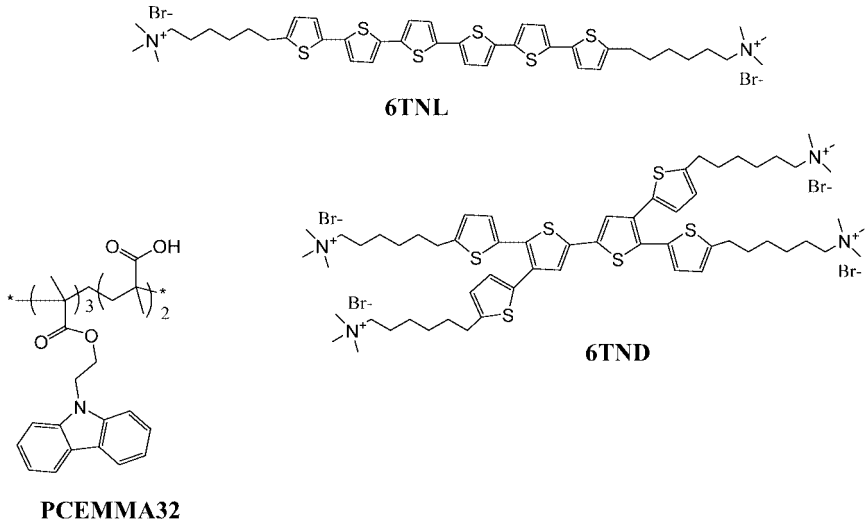

Figure 1. Chemical structures of the oligomers and polyelectrolyte used for fabrication of the nanostructured layer-by-layer films.

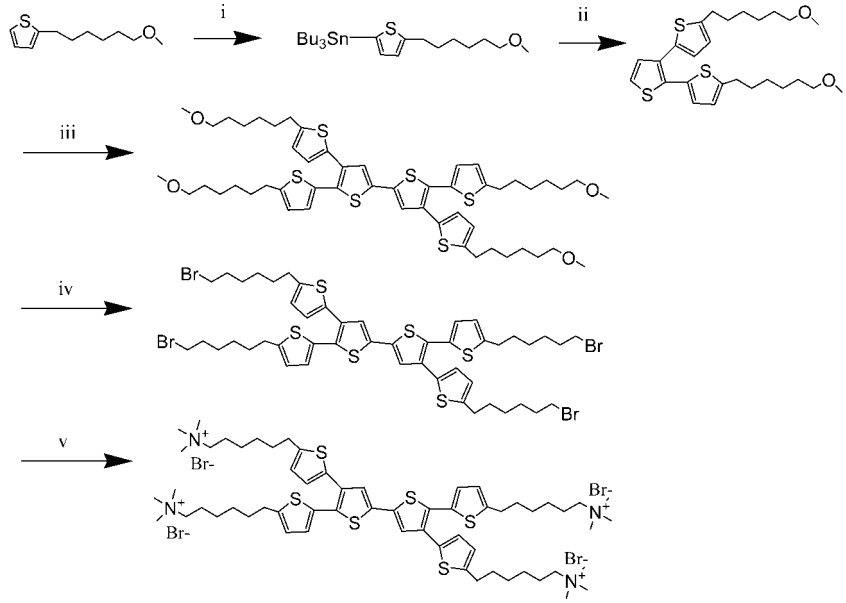

Figure 2. Synthesis scheme for 6TND. Reagents and conditions: (i) *n*-BuLi, THF, Bu_3SnCl, −78 °C to room temperature; (ii) 2,3-dibromothiophene, DMF, $Pd(PPh_3)_4$, 100 °C; (iii) *n*-BuLi, THF, $CuCl_2$; (iv) aqueous HBr, refluxing; and (v) trimethylamine, EtOH, refluxing.

then rinsed with DMSO/water (2/3) at pH 10 for 2 min. The substrates were then neutralized by rinsing with water for 30 s. (2) The substrates were immersed into the aqueous 6TNL or 6TND solutions (1 mg/mL) for 10 min and then rinsed with water for 2 min.

The alternate LbL films of 6TNL or 6TND with PCEMMA32 were achieved by repeating this process until the desired number of layers was reached. Figure 3 shows the composition and proposed structure of alternating multilayer films. For SPR measurements, the functionalized Au-coated LaSFN9 substrate was first dipped into the cationic sexithiophene solution, followed by the PCEMMA32 solution.

Instruments. UV−vis spectra were recorded using an Agilent 8453 UV−visible spectrometer. The thickness and the kinetic of adsorption for layer-by-layer films were measured by in situ SPR spectroscopy with gold-coated LaSFN9 glass substrate. The surface plasmon spectra were obtained in the SPR mode of the Multiskop instrument with the attenuated total reflection (ATR) setup used for the excitation of surface plasmons in the classical Kretschmann configuration.[28] For the electrochemical measurements, the potentiostat (Princeton Applied Research Parstat 2263) with three

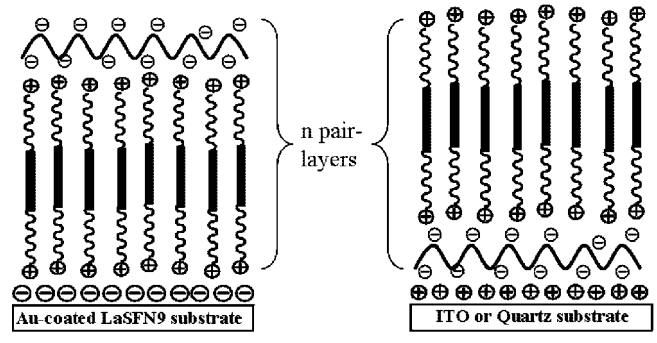

Figure 3. Schematic view of alternating LbL multilayer film buildup of 6TNL or 6TND with the precursor polyelectrolyte.

electrodes was used for cyclic voltammetry. Functionalized ITO substrate or gold-coated LaSFN9 glass substrate was used as the working electrode. The counter electrode was platinum wire with Ag wire as the reference electrode. The electrochemical cross-linking of layer-by-layer films was performed using 0.1 M $TBAPF_6$/acetonitrile as the supporting electrolyte. The solution was freshly

(28) Knoll, W. *MRS Bull.* **1991**, *16*, 29.

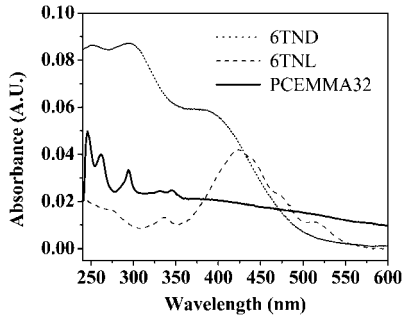

Figure 4. UV−vis absorption spectra of 6TNL and 6TND in water and PCEMMA32 in DMSO/water (2/3) at pH 10. The PL spectrum is shown in the Supporting Information.

purged with N_2 gas for 15 min prior to the experiment. Kinetic electrochemical cross-linking was studied using in situ EC-SPR. It was also used to monitor the oxidation/reduction and electrochemical properties of deposited films with reflectivity changes as a function of time. Details of the EC-SPR setup have been reported elsewhere.[18a,29] The excitation source employed was a He−Ne laser with $\lambda = 632.8$ nm on an ATR setup. The reflectivity-angular measurements were also performed by scanning an incident angle range before and after electrochemical cross-linking. The electrode surface area was 0.785 cm^2.

Results and Discussion

UV−Vis and Photoluminescence Spectra in Solution. Figure 4a shows the UV−vis absorption spectra of 6TNL and 6TND in water (5 μg/mL) and PCEMMA32 in water/DMSO (2/3) at pH 10. The dendritic sexithiophene shows spectroscopic properties that are different from those of the linear sexithiophene. The solution molar absorptivity was determined to be $\varepsilon_{max} = 7924$ M^{-1} cm^{-1} at $\lambda_{max} = 420$ nm for 6TNL and $\varepsilon_{max} = 16\,111$ M^{-1} cm^{-1} ($\lambda_{max} = 400$ nm) for 6TND. The λ_{max} chosen represented the longest conjugated α−α oligothiophene units corresponding to six (420 nm) and four (400 nm) thiophene units for 6TNL and 6TND, respectively. As previously described,[7a] there are two different linkages between each thiophene units including α,β and α,α linkages. The α,α linkage provides the best π-electron conjugation, while the α,β linkage disrupts it. The absorbance is directly proportional to molar absorptivity at constant concentration and path length (Beer−Lambert law). Another corollary is that, at a similar molar absorptivity, the higher concentration gives greater absorbance. Because of the more extended conjugation length with 6TNL, it was expected to have the higher molar absorptivity. However, the results indicate that even though 6TNL is expected to have a higher molar absorptivity, 6TND has more absorbance under 250−420 nm as well as higher molar absorptivity (also see the Supporting Information). The absorption spectrum of the dendrimeric 6TND is broad and shows three peaks at 385, 294, and 252 nm originating from the $\pi-\pi^*$ transitions, indicating a distribution of absorbing oligothiophene species. The lowest energy absorption at 400 nm is almost identical to that of α-quaterthiophene and represents the upper limit. This spectrum is reminiscent of the organic soluble 6T oligothiophene dendrimer previously reported.[7] Thus, the absorbance is a multiple of overlapping conjugated units of α,β and α,α connectivity, giving it a higher molar absorption. The absorption spectrum of 6TNL shows the strongest $\pi-\pi^*$ transition peak at 420 nm and several shoulders at 440, 470, and 515 nm. These distinct shoulders are due to the vibronic structure and/or Davydov interaction, indicating a degree of aggregation.[30] In fact, this vibronic structure disappears with the addition of 20% THF, the best solvent for 6TNL which has $\varepsilon = 10\,755$ ($\lambda_{max} = 442$ nm) almost similar to that of 6TND at $\lambda_{max} = 420$ nm (see the Supporting Information).[5a] As shown in Figure 1, 6TND and 6TNL have both hydrophobic sexithiophene units and cationic alkyl chain arms at the ends. The positively charged quaternized amine end-groups make the molecules hydrophilic and water soluble. However, 6TND has four quaternized amine end-groups which lead to greater water solubility compared to 6TNL. In addition, from previous studies,[5a] the shoulder peaks of 6TNL in water were found to originate from H-aggregation ($\pi-\pi$ stacking), which disappeared when THF was added (up to 30%). This phenomenon was not observed in the case of 6TND. The UV−vis absorption spectra of 6TND in different ratios of water/THF were identical, indicating that it is less prone to aggregation.

The above observations are also consistent with the solution photoluminescence (PL) spectra; that is, the PL spectrum can be observed for 6TND, but it was quenched for 6TNL in water (see the Supporting Information).[5a] The UV−vis spectrum of PCEMMA32 shows peaks at 245, 261, 293, 332, and 345 nm which were attributed to $\pi-\pi^*$ and $n-\pi^*$ transitions of the carbazole unit which presented as polymer pendant side groups.[31] The sloped baseline of the absorption may be due to some aggregation of PCEMMA32 in DMSO.

Multilayer Growth. Multilayer films of 6TNL and 6TND with PCEMMA32 on various substrates were fabricated by the LbL deposition technique. The layer deposition was monitored by UV−vis absorption spectroscopy on quartz substrates every two bilayers. Shown in Figure 5 is the UV−vis absorption spectra of the films prepared from 6TNL (a) and 6TND (b). The absorbance intensity of both 6TNL and 6TND increased linearly with increasing number of layers, indicating a stepwise and regular growth process. Shown in Figure 5c is the relationship between peak intensity at 238, 400, and 415 nm with the number of deposition layers for the two systems. It is evident that the stronger intensity at 238 nm is predominantly due to the incorporation of carbazole units from PCEMMA32, which is higher with the 6TND pairing. It is also clear that more 6TND units are incorporated per layer compared to 6TNL.

The peak at 400 nm, attributed to the oligothiophene units in water solution, is red-shifted to about 425 nm in the film which is due to the J-aggregation in the 6TND film. This is possibly due to a stronger electrostatic interaction between the dendrimeric sexithiophene and polycarbazole precursor molecule leading to a higher density of 6TND on the surface. For 6TNL in solution and film as seen from the shoulder peaks in solution, the aggregation of 6TNL was observed to be due to the H-aggregation (blue-shift). This shoulder disappeared in the film with the polycarbazole precursor molecule. This result is opposite to that of the 6TND aggregation phenomenon on the films.[23] The disappearance of these vibronic structure bands after adsorption with the polycarbazole precursor layer shows that deaggregation may have occurred during the adsorption process but also indicates a lower surface coverage for 6TNL consistent with our previous results.[5]

The kinetics of the layer-by-layer adsorption for both 6TNL and 6TND systems was studied by SPR at a fixed angle slightly lower than the resonance angle with water as the medium. The alternation of the layers between the cationic sexithiophenes and anionic polycarbazole precursor results in the buildup of

(29) Aust, E. F.; Ito, S.; Sawodny, M.; Knoll, W. *Trends Polym. Sci.* **1994**, *2*, 9.

(30) (a) Hotta, S.; Rughooputh, S. D. D. V.; Heeger, A.; Wudl, F. *Macromolecules* **1987**, *20*, 212. (b) Koren, A. B.; Curtis, M. D.; Kampf, J. W. *Chem. Mater.* **2000**, *12*, 1519.

(31) Fulghum, T.; Karim, S. M. A.; Baba, A.; Taranekar, P.; Nakai, T.; Masuda, T.; Advincula, R. C. *Macromolecules* **2006**, *39*, 1467.

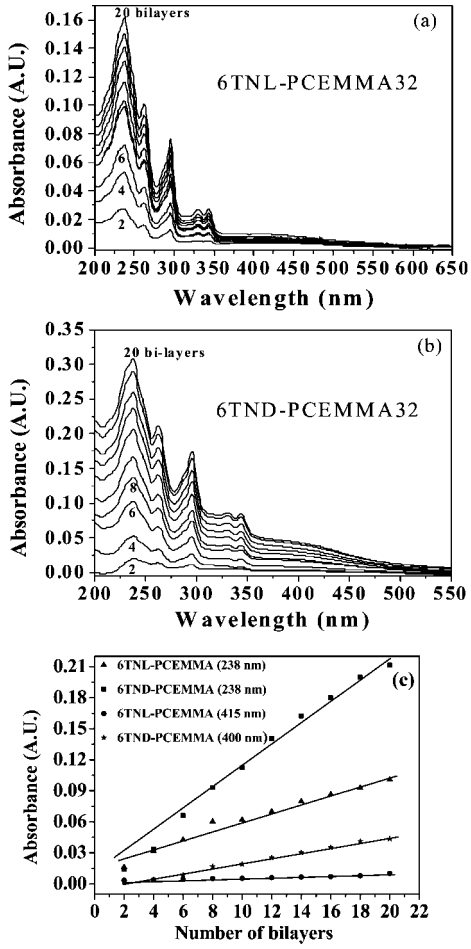

Figure 5. UV−vis spectra of (a) 6TNL-PCEMMA32 and (b) 6TND-PCEMMA32 multilayer films (up to 20 bilayers) and (c) plots of absorbance at 238 nm (from PCEMMA), 415 nm (from 6TNL), and 400 nm (from 6TND) versus the number of bilayers in both systems.

multilayers. SPR measurements allow for the in situ monitoring of film architecture while in contact with the aqueous medium. As shown in Figure 6, the adsorption kinetic curves of 6TNL (a) and 6TND (b) alternated with the adsorption of PCEMMA32 for 10 bilayers. At $t = 0$, the first aqueous solution of cationic sexithiophene 6TNL or 6TND was injected into the SPR cell with negatively functionalized gold and the adsorption was followed in real time. Each layer adsorption process was completed after several minutes. The reflectivity increases for every layer of sexithiophene added, indicating the deposition of these sexithiophenes. After 10 min, the film was simultaneously rinsed with water for 2 min, resulting in decreased reflectivity. The negatively charged PCEMMA32 was then injected and allowed to adsorb for 10 min. The film was again rinsed with water/DMSO (2/3) for 2 min and then neutralized with water for a further 30 s. This deposition protocol was repeated until the desired number of layers was reached. The insets show the actual SPR reflectivity-angular measurements before and after deposition. In general, an increase in overall thickness was observed for both systems.

Angular scan measurements were taken after every bilayer deposition in water for sexithiophenes and in water/DMSO (2/3) for PCEMMA32 in situ. The dip angles were shifted to higher incidence angles with increasing number of layers as shown in the inset of Figure 6. The film thickness was calculated by fitting these experimental SPR curves with a Fresnel equation algorithm (Winspall software version 2.20). The plots of the thickness as

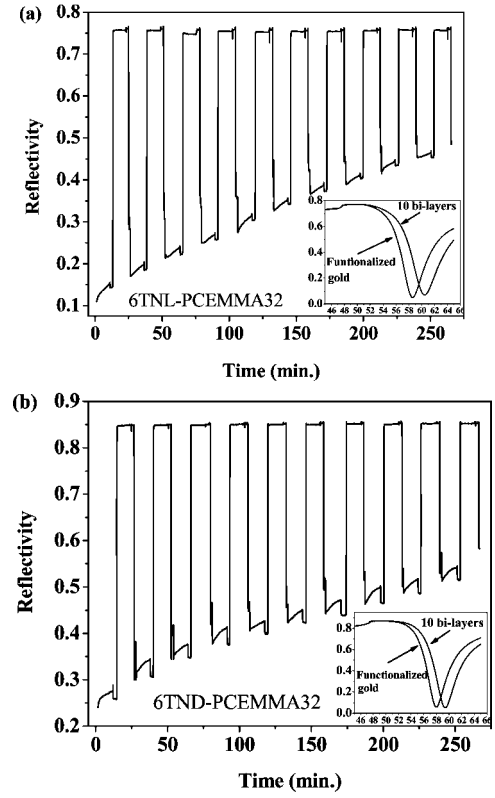

Figure 6. Time-dependent SPR experiments with 10 bilayers of (a) 6TNL/PCEMMA32 and (b) 6TND/PCEMMA32. The insets are the angle shifts after deposition.

a function of number of layers for both 6TNL and 6TND system were obtained (see the Supporting Information). The linear and stepwise increase of thickness with each layer in the 6TNL system was observed, consistent with the increase in UV−vis absorbance. The total film thickness is 177 Å after 10 bilayers as measured in situ or an average of 17.7 Å/pair-layer. For the 6TND system, the total film thickness is 180 Å after 10 bilayers or an average of 18.0 Å/pair-layer as measured in situ. As mentioned in a previous work,[23,32] the substrates can be predeposited with three-pair layers of polyelectrolytes (PSS/PDADMAC) to ensure the maximum surface charge density prior to deposition of their materials. What is interesting is that although the average/pair layer thickness is about the same, the higher absorbance intensity/layer for the 6TND/PCEMMA32 films indicates a higher chromophore density for these layers. This was confirmed by electrochemistry results as discussed in the following section. Other studies will also be required to prove the molecular orientation and morphology of the films which are important factors for eventual device fabrication and application.

Electropolymerization of Multilayer Films. The 20 bilayer films of both 6TNL/PCEMMA32 and 6TND/PCEMMA32 were fabricated on ITO substrates to investigate intralayer electropolymerization and cross-linking of carbazole units within the PCEMMA32 layers. Recently, our group[21c,31] reported the electropolymerization and cross-linking of poly(vinyl-*N*-carbazole) through the carbazole unit as the pendant side group. Figure 7a shows a schematic diagram of the electropolymerization and cross-linking of the carbazole unit. Shown in Figure 7 are the cyclic voltammetry (CV) traces of 6TNL/PCEMMA32 (Figure 7b) and 6TND/PCEMMA32 (Figure 7c). The electrochemical experiment was performed in 0.1 M $TBAPF_6$/acetonitrile electrolyte at a

(32) Locklin, J.; Shinbo, K.; Onishi, K.; Kaneko, F.; Bao, Z.; Advincula, R. C. *Chem. Mater.* **2003**, *15*, 1404.

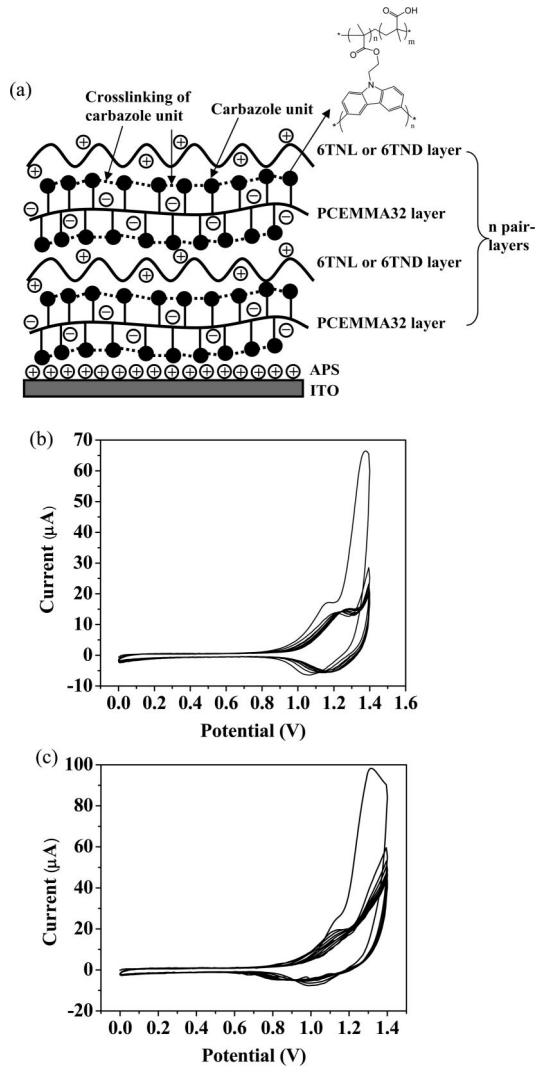

Figure 7. (a) Schematic diagram of electropolymerization and cross-linking of the carbazole unit, and CV traces of 10 cycles of (b) 6TNL/PCEMMA32 and (c) 6TND/PCEMMA32 layer-by-layer deposition films at a scan rate of 20 mV/s.

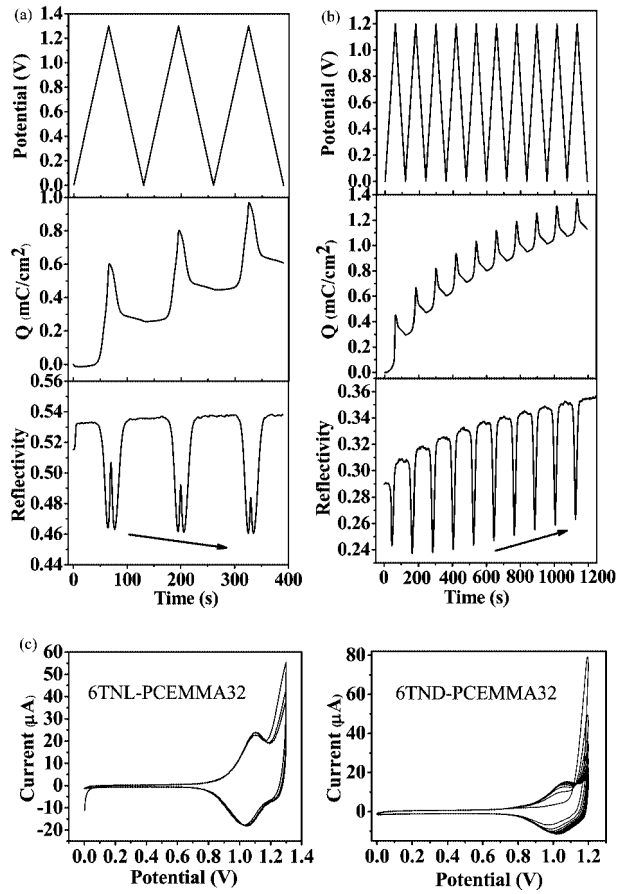

Figure 8. EC-SPR results: (a and b) potential ramp (top), amount of charge (middle), and kinetic curve (bottom) during electropolymerization (cross-linking) of polycarbazole precursor layers on 6TNL and 6TND films in 0.1 M $TBAPF_6$/acetonitrile and (c) corresponding CV traces.

scan rate of 20 mV/s. The potential was cycled from 0 to 1.4 V for 10 cycles with Ag wire as the reference electrode and Pt wire as the counter electrode. The electrochemical process with the 6TNL system was reversible, indicating that the electroactive carbazole unit was easily oxidized in the 6TNL system. From the CV trace of 6TNL, the first cycle shows an oxidation onset peak at ~1.37 V and shifts to 1.4 V with subsequent cycles. The oxidation doping peak appears at ~1.16 V and shifts to ~1.27 V with subsequent cycles. The appearance of this oxidation doping peak indicated the cross-linking of carbazole units in PCEMMA32 layers. The corresponding reduction-dedoping peak appears at ~1.05 V in the first cycle and shifts to ~1.2 V with subsequent cycles. On the other hand, as seen in the CV trace of 6TND, the oxidation onset peak for the first cycle appears at ~1.32 V and shifts to 1.4 V with subsequent cycles. The oxidation doping peak appears at ~1.1 V with the corresponding reduction-dedoping peak at ~1.0 V. By comparison, for the 6TND films, the current due to doping was higher than that of the 6TNL film, indicating the 6TND film is more electrochemically active or contains more chromophore. Nevertheless, the doping−dedoping currents increased with each cycle for both systems. After electropolymerization, the UV−vis spectra of the films were compared with those of the films before electropolymerization. The carbazole peaks at ~330 and ~345 nm disappeared and a new peak at ~400 nm was observed which overlapped with the oligothiophene peak. The appearance of this red-shifted peak is due to the formation of more conjugated PCEMMA32 (conversion to polycarbazole) after electropolymerization.[25,26] These confirmed the cross-linking of carbazole units within the PCEMMA32 layers in both systems. Note that the contribution of oligothiophene redox couples are present but should be overlapped by the carbazole and polycarbazole redox peaks, as oligothiophene usually does not have very strong redox peaks in this region.[33]

Electrochemical Surface Plasmon Resonance Spectroscopy (EC-SPR). The combination of SPR and electrochemical CV allowed for the in situ (kinetic) investigation of the changes in the dielectric constant and/or thickness of the LbL film during the doping−dedoping or protonation−deprotonation processes.[34] The EC-SPR experiments were performed in the same condition corresponding to that of the previous CV experiments. The 10 bilayers of both systems were fabricated in situ on gold-coated LaSFN9 glass substrates and incorporated in an electrochemical cell ATR setup. The kinetic trend of the electropolymerization process including potential ranges (top), amount of charge (middle), and reflectivity changes (bottom) of the deposited 6TNL/PCEMMA32 and 6TND/PCEMMA32 films are shown in Figure 8a and b. The data were recorded as a function of time (up to 3 cycles for 6TNL and 10 cycles for 6TND systems).

(33) Zotti, G.; Randi, A.; Destri, S.; Porzio, W.; Schiavon, G. *Chem. Mater.* **2002**, *14*, 4550.

(34) Baba, A.; Park, M.-K.; Advincula, R. C.; Knoll, W. *Langmuir* **2002**, *18*, 4648.

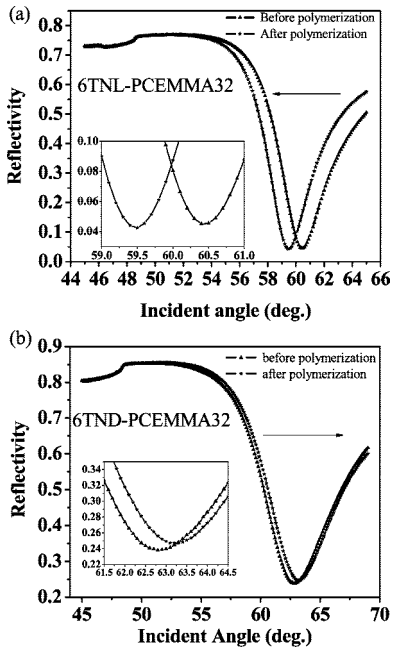

Figure 9. Angular scan measurements of electropolymerized films (a) 6TNL and (b) 6TND.

The potential cycling was 0−1.3 V for 6TNL system and 0−1.2 V for the 6TND system as shown in Figure 8c. The stepwise increase of reflectivity was observed after each potential cycling. For the 6TNL system, the reflectivity in the anodic scan gradually increases and then rapidly decreases at ∼1.0 V which relates to the oxidation doping peak at ∼1.0 V as shown in the CV trace. The reflectivity again increases to a maximum at 1.3 V which corresponds to the other oxidation onset peak at 1.3 V. The rapid increase of reflectivity was also observed in the cathodic scan. However, with an increasing number of cycles, the net maximum reflectivity decreases stepwise.

In general, a decrease and increase in reflectivity were observed during the oxidation−doping and reduction−dedoping processes, respectively, for both films. The changes in reflectivity occur due to the fact that the thickness or the dielectric constant is changing.[21] Since the overall change in reflectivity is higher for the 6TND/PCEMMA system, this indicated the formation of a thicker film or a higher dielectric constant trend. The amount of charge tracks the electron transfer between carbazole units and electrode for both systems (middle panel of Figure 8a and b). It showed an increase during the doping process and a decrease during the dedoping process. In this case, the amount of charge/cycle for 6TNL/PCEMMA32 is higher than that for 6TND/PCEMMA32. This means the 6TNL/PCEMMA32 film ultimately gives a higher degree of cross-linking or doping effect for PCEMMA32. Consistent with the changes in reflectivity and amount of charge, it can be concluded that the 6TND/PCEMMA32 films have a greater electrochromic effect than the 6TNL/PCEMMA32 films but have a less effective cross-linking environment for the precursor layers. This could be a consequence of greater electron tunneling through the less dense 6TNL layers, rendering an effective cross-linking stage for the PCEMMA32 layers. This is not unfounded, since 6TND has been shown to form more dense layers based on stronger electrostatic interaction with the precursor layers, and this was confirmed by UV−vis and SPR thickness measurements.

After the electropolymerization, the electropolymerized films were characterized by SPR reflectivity-angular scans. As shown in Figure 9, the incident angle shifts to a lower angle for the 6TNL film (Figure 9a) and higher angle for the 6TND film (Figure 9b). Two possible explanations for the different shift trends in the SPR angular scan curves can be considered.[19b,34,35] The first explanation is that the thickness of the films changed differently after polymerization. The thinner film is a result of cross-linking of the precursor layers on the 6TNL/PCEMMA32 films which causes thickness contraction as shown by EC-SPR. For the 6TND film, this resulted in thicker films (opposite trend) based on an increased volume due to the several doping−dedoping process cycles and a lower degree of cross-linking. The second explanation is that this is due to the change in the real (ε') and imaginary (ε'') parts of the dielectric constant of the films. In general, from the experimental data, the overall film SPR reflectivity was found to increase during the oxidation−doping process and to decrease during the reduction−dedoping process. A net decrease could indicate that the electropolymerized 6TNL film will have a higher dielectric constant based on more cross-linked polycarbazole units formed whereas the 6TND film ends up incorporating more void space during repeated CV cycling, resulting in a lower dielectric constant. These differences can again be a consequence of the higher density of the 6TND layers compared to the 6TNL layers which allowed greater electropolymerizability/cross-linking of the PCEMMA32 layers. Thus, these layers when cross-linked will contract and prevent effective film swelling during the doping−dedoping cycles. The net effect is a decrease in overall film thickness as observed for the 6TNL/PCEMMA32 system.

Conclusion

Alternate LbL films of cationic 6TNL and 6TND with anionic PCEMMA32 were fabricated on several substrates which exhibited linear growth as monitored by UV−vis spectroscopy and in situ SPR spectroscopy. The alternate precursor PCEMMA32 layers were found to be electropolymerizable. The electrochemical and electrochromic properties were consistent with the formation of an intralayer CPN formation as observed by CV and in situ EC-SPR spectroscopy. Thus, the pendant carbazole unit in the PCEMMA32 layer was electropolymerized to form polycarbazole species with a reversible oxidation−reduction process. EC-SPR confirmed the reversible doping−dedoping process and electrochromic effect. After cross-linking, the angular-reflectivity measurements resulted in shifts to lower and higher angles for the 6TNL and 6TND systems, respectively. These results can be mainly attributed to the changes in the dielectric constant and thickness for these films after electropolymerization which are influenced by the density and ordering of the 6TNL and 6TND layers and the electropolymerizability of the PCEMMA32 layers. In the future, these films can be optimized for specific hole-transport and charge-carrier mobility applications based on controlled ordering and electropolymerizability of the layers.

Acknowledgment. The authors gratefully acknowledge partial funding from the Robert E. Welch Foundation (E-1551), NSF DMR-0602896 and NSF-CTS 0330127. The authors also acknowledge partial funding support from Faculty of Science and Graduate School, Chiang Mai University. S.S. would like to thank the Commission on Higher Education, Ministry of Education, Thailand for a research scholarship.

Supporting Information Available: Experimental details for the synthesis of 6TND and PL spectra of 6TNL and 6TND in different solvent mixtures, SPR ex situ measurements, and thickness correlation. This material is available free of charge via the Internet at http://pubs.acs.org.

LA800307U

(35) Baba, A.; Advincula, R. C.; Knoll, W. *J. Phys. Chem. B* **2002**, *106*, 1581.